10^{-12} m^2 N^{-1}; the data for copper are given in parentheses. The stress was assumed to be uniaxial and parallel to the rolling direction. Angle $\varphi = 0$. The diffraction strain was calculated for the 112 reflection in steel and the 224 reflection in copper. The results for steel are given in Fig. 1 and for copper in Fig. 2. The straight line gives the results for the texture-free materials; the curves are the results for the actual materials.

Our conclusion is that in practical cases the presence of texture may lead to an amplitude of the oscillations in d_{HKL} *vs* $\sin^2 \psi$ that is of the same order of magnitude as the diffraction strain itself.

References

BRAKMAN, C. M. (1985*a*). *Cryst. Res. Technol.* **20**, 593-618.

BRAKMAN, C. M. (1985*b*). Unpublished research.

BUNGE, H. J. (1982). *Texture Analysis in Materials Science.* London: Butterworths.

DÖLLE, H. (1979). *J. Appl. Cryst.* **12**, 489-501.

DÖLLE, H. & HAUK, V. (1977). *Z. Metallkd.* **68**, 719-724.

HAUK, V. (1955). *Z. Metallkd.* **46**, 33-38.

HAUK, V. M. (1984). *Adv. X-ray Anal.* **27**, 101-120.

JAMES, M. R. & COHEN, J. B. (1980). *The Measurement of Residual Stresses by X-ray Diffraction Techniques.* In *Experimental Methods in Materials Science*, Vol. 1, edited by H. HERMAN, pp. 1-62. New York: Academic Press.

MACHERAUCH, E. & MÜLLER, P. (1961). *Z. Angew. Phys.* **13**, 305-312.

Acta Cryst. (1988). A**44**, 163-167

Non-linear Diffraction Strain *vs* $\sin^2 \psi$ Phenomena in Specimens Exhibiting Rolling-Type Texture

BY C. M. BRAKMAN AND P. PENNING

Delft University of Technology, Laboratory of Metallurgy, Rotterdamseweg 137, 2628 *AL Delft, The Netherlands*

(*Received* 28 *April* 1987; *accepted* 1 *October* 1987)

Abstract

Non-linearities in measured diffraction strains are frequently observed in textured materials. For the case of textured cold-rolled low-carbon steel sheet specimens the diffraction strain is analysed in its constituents: single-crystallite strain and the orientation distribution function of the crystallites. With only *macro*-stresses σ_1 and σ_2 taken into account, a satisfactory explanation of practical measurements on these steel specimens is obtained.

1. Introduction

The '$\sin^2 \psi$ method' (Hauk, 1955; Macherauch & Müller, 1961; Dölle & Hauk, 1977; Dölle, 1979; James & Cohen, 1980; Hauk, 1984; Hauk & Macherauch, 1984) is used to determine (residual) stresses from diffraction data. The measured diffraction line-shift strain often exhibits straight-line behaviour when plotted *vs* $\sin^2 \psi$. From intercepts and slopes the stresses may be calculated. The symbol ψ stands for the angle between the scattering vector and the specimen's normal direction (ND). The symbol φ is used for the angle between the projection of the scattering vector on the plane of the specimen and rolling direction (RD).

In *textured* specimens, significant deviations from linearity frequently occur (Faninger & Hauk, 1976; Hauk, Herlach & Sesemann, 1975; Hauk & Sesemann, 1976; Hauk & Kockelmann, 1977, 1978; Marion & Cohen, 1977; Hauk, Krug & Vaessen, 1981; Dölle & Cohen, 1980; Hauk & Vaessen, 1985; Hauk, Vaessen & Weber, 1985; Maurer, Neff, Scholtes & Macherauch, 1987). These reports concern cold-rolled steel sheets and $\varphi = 0$. Small or negligible non-linearities are reported for measurements in the plane $\varphi = \pi/2$. Examples are given in Figs. 1 and 2. In all cases the 211 reflection was used.

It is the purpose of this paper to clarify the physical nature of this non-linear diffraction strain behaviour for textured cold-rolled low-carbon steel specimens using the 211 reflection. The specimens are considered to be single phase. The orientation distribution function (o.d.f.) of the crystallites (Bunge, 1982) offers a quantitative description of crystallographic texture. Diffraction strain is an o.d.f.-weighted average of all single crystallite strains of the grains engaged in the diffraction. The o.d.f. depends in an irregular way on ψ and φ. Accordingly, linear diffraction strain behaviour with respect to $\sin^2 \psi$ cannot be expected. It is shown that the behaviour of the o.d.f.'s of cold-rolled steel leads to diffraction strain phenomena measured in practice.

An assumption has to be made concerning the stress state of the specimen. Only principal stresses σ_1 and σ_2 are considered. They operate parallel to the rolling

0108-7673/88/020163-05$03.00

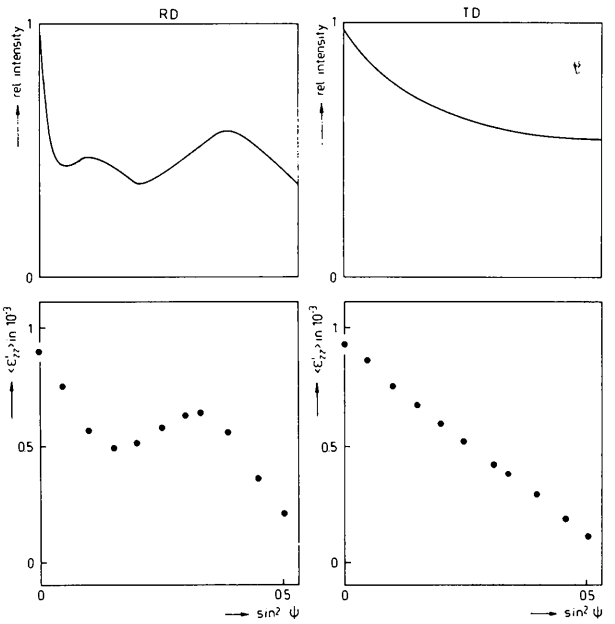

Fig. 1. Measured 211 relative intensities (upper figures) *vs* $\sin^2 \psi$ for $\varphi = 0$ (left-hand figures) and $\varphi = \pi/2$ (right-hand figures). Specimen: low-carbon steel reduced 75% by cold rolling. After Dölle & Cohen (1980). RD = rolling direction; TD = transverse direction.

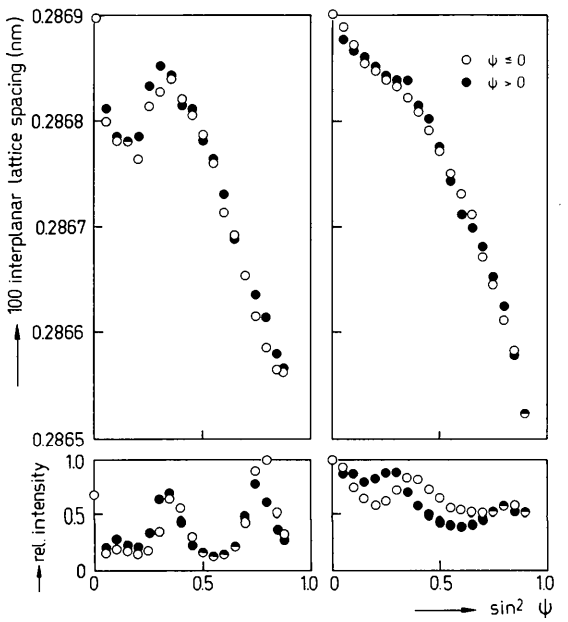

Fig. 2. Measured relative intensities (lower figures) and interplanar lattice spacing for angles $\varphi = 0$ (left-hand figures) and $\varphi = \pi/2$ (right-hand figures). 211 reflection used but interplanar lattice spacing converted to (100) spacing. Specimen: low-carbon structural steel reduced 75% by cold rolling. Solid circles: positive ψ angles; open circles: negative ψ angles. Absence of ψ splitting. After Hauk, Vaessen & Weber (1985). Diffraction strain 'oscillation' for $\varphi = 0$; approximate straight-line behaviour for $\varphi = \pi/2$ in both Figs. 1 and 2.

direction (RD) and transverse direction (TD), respectively. These stresses are taken to be macro-stresses. No use is made of the so-called stresses of the second kind (Macherauch, Wohlfahrt & Wolfstieg, 1973) for the explanation of non-linearity (Hauk, Vaessen & Weber, 1985; Maurer *et al.*, 1987). It is shown that crystallographic texture in conjunction with macro-stresses σ_1 and σ_2 offers an explanation of cold-rolled steel non-linear diffraction strain phenomena.

2. Theoretical

It has been shown in the previous paper (paper I) (Penning & Brakman, 1988) that, for the case of $m3m$ crystals in conjunction with the 211 reflection, only one trace in orientation space needs to be considered [$t = 1$ in equation (12), paper I]. In what follows only the measurement planes $\varphi = 0$ and $\varphi = \pi/2$ are taken into account.

In paper I, both single-crystallite strain and the orientation distribution function (o.d.f.) of the crystallites are written as Fourier series with respect to the rotation angle about the scattering vector, φ_2''.

2.1. *Single-crystallite strain*

The Fourier series of the dilatation in spacing d_{hkl} of a crystallite with [*hkl*] parallel to the scattering vector only exhibits five terms: equation (9), paper I. The values of χ, Γ, A, N and E_{k1} to E_{k4} can be determined from equations (3) and (10) and Table 6 of paper I and the E_{k0} are defined (only σ_1 and $\sigma_2 \neq 0$) by

$$\sum_{k=1}^{2} E_{k0}\sigma_k = s_{12}^{\text{eff}}(hkl)(\sigma_1 + \sigma_2) + \tfrac{1}{2}s_{44}^{\text{eff}}(hkl)(\sigma_1 \cos^2 \varphi + \sigma_2 \sin^2 \varphi) \sin^2 \psi, \quad (1)$$

where s_{12}^{eff} and $\frac{1}{2}s_{44}^{\text{eff}}$ have been defined in paper I.

It can be shown that, for $\varphi = 0$ and $\varphi = \pi/2$, $E_{11} = E_{21} = E_{14} = E_{24} = 0$. For the 211 reflection, $\chi = 0$. Consequently, the coefficients of $\cos \varphi_2''$ and $\sin 2\varphi_2''$ in equation (9), paper I, equal zero. Of the five Fourier coefficients only three remain: $(\varepsilon'_{zz})_0$, $(\varepsilon'_{zz})_2$ and $(\varepsilon'_{zz})_3$ of equation (12), paper I. They are connected to $\cos 0\varphi_2''$, $\sin \varphi_2''$ and $\cos 2\varphi_2''$, respectively.

In Figs. 3(*a*), (*b*) and 4, these Fourier coefficients are given as a function of $\sin^2 \psi$ for the case of Fe crystals. Two stress states are considered: $\sigma_1 = -\sigma_2$ and $\sigma_1 = \sigma_2$.

2.2. *The orientation distribution function (o.d.f.) of the crystallites*

In Table 2 of Brakman (1985*b*), the Fourier coefficients of the o.d.f. with respect to the angle φ_2' are given. The relationship between φ_2' and φ_2'' of the present paper is given by $\varphi_2'' = \varphi_2' + \arg z_1(hkl)$. In the Fourier coefficients the texture-dependent functions

$C_j^{\mu}(\psi, \varphi)$ and $E_j^{\mu}(\psi, \varphi)$ also occur. They are equal to zero for both $\varphi = 0$ and $\varphi = \pi/2$. Their definition and that of arg z_1 is given in equations (II-13), (II-15) and (I-9/10), respectively, of Brakman (1985*b*). Rearrangement of the Fourier coefficients with respect to φ_2'' leads to the result that, for the φ angles mentioned, the o.d.f.'s Fourier coefficients* connected to cos φ_2'' and sin $2\varphi_2''$ equal zero for the 211 reflection.

Consequently, in equation (12), paper I, only the Fourier coefficients D_0, D_2 and D_3 need to be considered. In Figs. 5(*a*) and (*b*), D_0, D_2 and D_3 of a cold-rolled steel texture are depicted *vs* sin^2 ψ for $\varphi = 0$ and $\varphi = \pi/2$. It follows that the $\varphi = 0$ o.d.f. Fourier coefficients oscillate more strongly with respect to sin^2 ψ than the $\varphi = \pi/2$ coefficients do. Note that D_0 is equal to the (normalized in terms of 'times random') measured intensity.

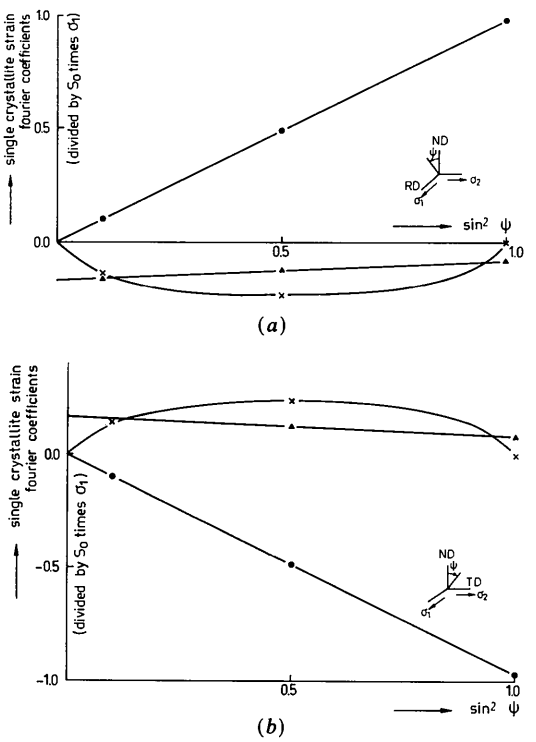

Fig. 3. Fourier coefficients *vs* sin^2 ψ of Fe single-crystallite strain for $\varphi = 0$ (*a*) and $\varphi = \pi/2$ (*b*). [112] parallel to scattering vector, *i.e.* the ψ, φ direction. Single-crystallite strain Fourier series according to equation (9) of paper I. Stress state assumed: $\sigma_1 = -\sigma_2$; other stresses equal to zero. σ_1 parallel to rolling direction; σ_2 parallel to transverse direction of rolled sheet. ●: zero-order Fourier coefficient; ×: coefficient of sin φ_2''; ▲: coefficient of cos $2\varphi_2''$. Fourier coefficients divided by s_0 times σ_1.

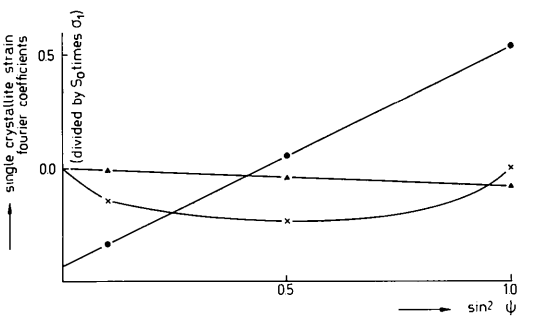

Fig. 4. Single-crystallite strain Fourier coefficients *vs* sin^2 ψ. As Fig. 3 but stress state $\sigma_1 = +\sigma_2$. Figure applies to all φ angles. The single-crystallite strains and consequently their Fourier coefficients, for two φ angles $\pi/2$ rad different from each other, are related by $\varepsilon'_{zz}(\psi, \varphi, hkl, \varphi_2'', \eta) = \eta\varepsilon'_{zz}(\psi, \varphi + \pi/2, hkl, \varphi_2'', 1/\eta)$, where $\eta = \sigma_2/\sigma_1$.

* For specimen symmetries lower than orthorhombic this only holds for $\varphi = 0$.

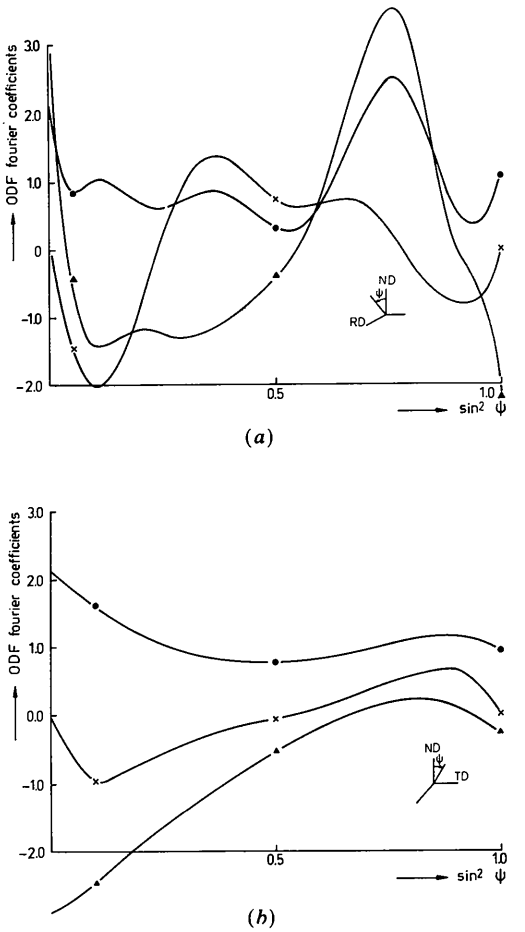

Fig. 5. Fourier coefficients D_0, D_2 and D_3 *vs* sin^2 ψ of the cold-rolled steel o.d.f. for $\varphi = 0$ (*a*) and $\varphi = \pi/2$ (*b*). [112] parallel to scattering vector, *i.e.* the ψ, φ direction. O.d.f. coefficients according to equation (12), paper I. ●: zero-order coefficient D_0; ×: coefficient D_2 of sin φ_2''; ▲: coefficient D_3 of cos $2\varphi_2''$. $\varphi = 0$ coefficients oscillate more strongly *vs* sin^2 ψ than the $\varphi = \pi/2$ coefficients. Specimen: low-carbon steel sheet reduced 64% by cold rolling. Details of o.d.f: Brakman (1985*a*). D_0 equals the pole-figure intensity in the ψ, φ direction. Compare D_0 with the intensity graphs of Figs. 1 and 2.

3. Results and discussion

A synthesis according to equation (12), paper I, of single-crystallite strain and o.d.f. Fourier coefficients is given in Figs. 6 and 7. The o.d.f. of the cold-rolled steel specimen used has been given elsewhere (Brakman, 1985*a*). The two macro-stress states $\sigma_1 = -\sigma_2$ and $\sigma_1 = \sigma_2$ are dealt with in Fig. 6 and Fig. 7 respectively. All other stress-tensor elements have been taken equal to zero.

The heavy curved lines in the graphs represent the mean diffraction strain according to equation (12), paper I. The single-crystallite strain distribution with respect to the rotation angle φ_2'' exhibits a minimum and a maximum. For every orientation of the scattering vector, the extremal crystallite strains are represented by the thin upper and lower curved lines. The diffraction strain is the o.d.f.-weighted average of the single-crystallite strains. Therefore, the diffraction strain curve is always between the extremal strain curves. The straight line represents the texture-free (Reuss model) diffraction strain, *i.e.* $(\varepsilon_{zz})_0$. The single-crystallite strain data were calculated using the Fe compliances: $s_{11} = 7{\cdot}57$, $s_{12} = -2{\cdot}82$ and $s_{44} = 8{\cdot}64$ (10^{-12} m^2 N^{-1}). Both diffraction and single-crystallite strain in Figs. 6 and 7 have been divided by the elastic anisotropy s_0 times σ_1.

In both Figs. 6 and 7 the $\varphi = \pi/2$ diffraction strain graphs exhibit small oscillations with respect to the texture-free straight line as compared with the $\varphi = 0$ case. This also holds for other stress states (not shown). Evidently, this is a consequence of the behaviour of the o.d.f. Fourier coefficients as depicted in Fig. 5. The single-crystallite strain Fourier coefficients only have a small influence since they behave smoothly with respect to $\sin^2 \psi$.

Deformation textures of steel develop almost irrespective of chemical composition and processing

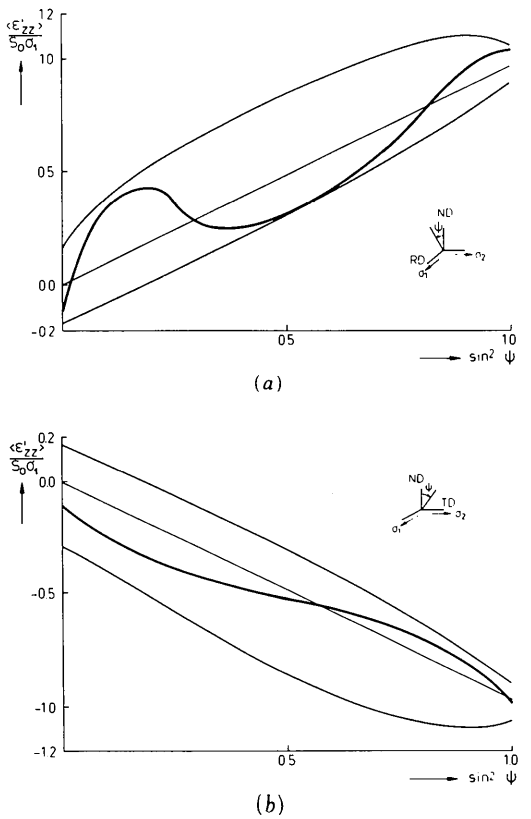

Fig. 6. Calculated 211 diffraction strain *vs* $\sin^2 \psi$ for $\varphi = 0$ (*a*) and $\varphi = \pi/2$ (*b*) for stress state $\sigma_1 = -\sigma_2$. Heavy curved lines: synthesis of Figs. 3 and 5 according to equation (12), paper I. Straight lines: texture-free diffraction strain. Reuss model of elasticity. All strains divided by s_0 times σ_1. Thin curved lines: minimal and maximal values of single-crystallite strain distributions with respect to rotation angle about the scattering vector. Diffraction strain as an o.d.f.-weighted average of single-crystallite strains is contained within these extremal strain curves. The vertical distance between the extremal strain curves represents theoretical line breadth. Note that the $\sigma_1 = -\sigma_2$ case yields a larger line breadth than found for $\sigma_1 = +\sigma_2$.

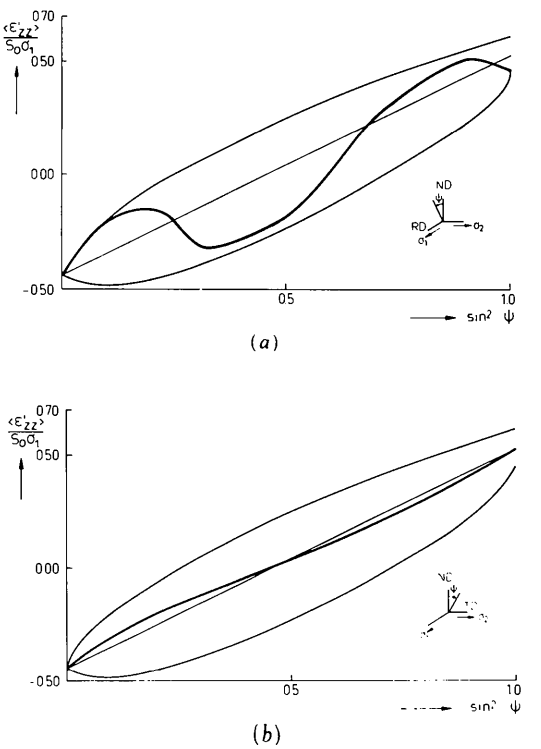

Fig. 7. As Fig. 6, but 211 diffraction strain *vs* $\sin^2 \psi$ for $\varphi = 0$ (*a*) and $\varphi = \pi/2$ (*b*) for stress state $\sigma_1 = +\sigma_2$. Strains divided by s_0 times σ_1. The literature (Hauk, Vaessen & Weber, 1985; Dölle & Cohen, 1980; Maurer *et al.*, 1987) reports a biaxial *compressive* stress state after cold rolling of low-carbon steels. On multiplication of (*a*) and (*b*) by s_0 times negative σ_1, a close approximation of Figs. 1 and 2 is obtained. The oscillations are predicted very well. However, the amplitudes are too large. They can be reduced by adopting the Hill (1952) approximation and averaging the Reuss- and Voigt-model results. A fit to practical measurements can be obtained allowing departures from the $|\sigma_1| = |\sigma_2|$ condition and using the magnitudes of σ_1 and σ_2 as fitting parameters.

conditions. Therefore, a comparison of Figs. 6 and 7 with the measured diffraction strain data of Figs. 1 and 2 (obtained on similar but not identical steels) is possible.

For cold-rolled steels a compressive biaxial stress state results (Dölle & Cohen, 1980; Hauk, Vaessen & Weber, 1985; Maurer *et al.*, 1987) exhibiting approximately equal σ_1 and σ_2 values. Multiplying Fig. 7 by -1, it follows that the $\eta = +1$ graphs indeed strongly resemble the measured curves of Figs. 1 and 2. Differences may be due to deviations from $\eta = +1$, different actual magnitudes of σ_1 and/or σ_2 and small texture differences.

The essence, however, is that macro-stresses σ_1 and σ_2 in conjunction with crystallographic texture qualitatively explain the non-linearities observed. No use has to be made of other stress-tensor elements or the so-called stresses of the second kind (Macherauch *et al.*, 1973).

The authors express their gratitude towards Dr Ir Th. H. de Keijser and Mr N. M. van der Pers for providing X-ray diffraction facilities.

The support of Dr P. van Houtte and Mr M. Mine of the Catholic University Leuven, Belgium, is gratefully acknowledged.

References

BRAKMAN, C. M. (1985*a*). *Cryst. Res. Technol.* **20**, 593-618.
BRAKMAN, C. M. (1985*b*). *J. Appl. Cryst.* **18**, 279-295.
BUNGE, H. J. (1982). *Texture Analysis in Materials Science.* London: Butterworths.
DÖLLE, H. (1979). *J. Appl. Cryst.* **12**, 489-501.
DÖLLE, H. & COHEN, J. B. (1980). *Metall. Trans. A*, **11A**, 831-836.
DÖLLE, H. & HAUK, V. (1977). *Z. Metallkd.* **68**, 719-724.
FANINGER, G. & HAUK, V. (1976). *Härterei-Tech. Mitt.* **31**, 98-108.
HAUK, V. (1955). *Z. Metallkd.* **46**, 33-38.
HAUK, V. (1984). *Adv. X-ray Anal.* **27**, 101-120.
HAUK, V., HERLACH, D. & SESEMANN, H. (1975). *Z. Metallkd.* **66**, 734-737.
HAUK, V. & KOCKELMANN, H. (1977). *Z. Metallkd.* **68**, 719-724.
HAUK, V. & KOCKELMANN, H. (1978). *Z. Metallkd.* **69**, 16-21.
HAUK, V., KRUG, W. H. & VAESSEN, G. (1981). *Z. Metallkd.* **72**, 51-58.
HAUK, V. & MACHERAUCH, E. (1984). *Adv. X-ray Anal.* **27**, 81-99.
HAUK, V. & SESEMANN, H. (1976). *Z. Metallkd.* **67**, 646-650.
HAUK, V. & VAESSEN, G. (1985). *Z. Metallkd.* **76**, 102-107.
HAUK, V., VAESSEN, G. & WEBER, B. (1985). *Härterei-Tech. Mitt.* **40**, 122-128.
HILL, R. (1952). *Proc. Phys. Soc. London Sect. A*, **65**, 349-354.
JAMES, M. R. & COHEN, J. B. (1980). *The Measurement of Residual Stresses by X-ray Diffraction Techniques.* In *Experimental Methods in Materials Science*, Vol. 1, edited by H. HERMAN, pp. 1-62. New York: Academic Press.
MACHERAUCH, E. & MÜLLER, P. (1961). *Z. Angew. Phys.* **13**, 305-312.
MACHERAUCH, E., WOHLFAHRT, H. & WOLFSTIEG, U. (1973). *Härterei-Tech. Mitt.* **28**, 201-211.
MARION, R. H. & COHEN, J. B. (1977). *Adv. X-ray Anal.* **20**, 355-367.
MAURER, G., NEFF, H., SCHOLTES, B. & MACHERAUCH, E. (1987). *Z. Metallkd.* **78**, 1-7.
PENNING, P. & BRAKMAN, C. M. (1988). *Acta Cryst.* **A44**, 157-163.

Acta Cryst. (1988). A**44**, 167-176

Distortion-Induced Scattering due to Vacancies in $NbC_{0.72}$

BY K. OHSHIMA* AND J. HARADA

Department of Applied Physics, Nagoya University, Nagoya 464, *Japan*

M. MORINAGA

Toyohashi University of Technology, School of Production Systems Engineering, Tempaku-cho, Toyohashi-shi, Aichi 440, *Japan*

AND P. GEORGOPOULOS AND J. B. COHEN

MATRIX and Department of Materials Science and Engineering, The Technological Institute, Northwestern University, Evanston, IL 60201, *USA*

(*Received* 23 *July* 1987; *accepted* 7 *October* 1987)

Abstract

The diffuse X-ray (and electron) scattering from $NbC_{0.72}$, previously thought to be due to vacancy octahedra, is shown to be dominated by the scattering due to mean-square atomic displacements with wave vectors near the Brillouin-zone boundary. The atomic displacements are similar to those produced by an optical phonon. On the basis of the sign and amplitude of the displacement parameters a model for the environment around a carbon vacancy is proposed.

* Present address: Institute of Applied Physics, University of Tsukuba, Sakura, Ibaraki 305, Japan.

0108-7673/88/020167-10$03.00